

Wormhole inducing inflation with Einstein Gauss Bonnet dilaton interaction

Gargi Biswas*, M K Dutta[†] and B Modak[‡]

December 3, 2021

^{*,‡} Department of Physics, University of Kalyani, Kalyani-741235, India.

[†] Department of Physics, BRSN College, Kolkata- 740120, India.

Abstract

We present a few Euclidean wormhole configurations using both the analytic and numerical solutions of the field equations considering Einstein Gauss-Bonnet dilaton interaction in 4-dimensional Robertson Walker Euclidean background. The analytic solutions in some cases show a transition to an exponential expansion with Lorentzian time t using $\tau = it$ after passing through an era of oscillating Euclidean wormhole. The numerical solutions of the scale factor $a(\tau)$ show multiple local maxima and minima about a global minimum for inverse power law potentials, while for exponential potential the wormholes have a single minimum. The Hubble parameter and deceleration parameter obtained by curve fit of $a(\tau)$ of the numerical solution show an inflation away from the throat of the wormhole invoking analytic continuation by $\tau = it$. A sharp decay of the potential is also observed.

PACS: 98.80.-k, 04.50.-h.

Keywords: Wormhole, Multiple maxima and minima, Inflation and Einstein Gauss-Bonnet dilaton interaction.

1 Introduction:

Inflationary cosmology [1–4] resolves most of the problems of standard cosmology, except cosmic singularity and vanishing of cosmological constant [5]. To avoid cosmic singularity in the early universe several gravitational theories, like modified theories of gravity [6–9], string theory [10, 11], Kaluza-Klein gravity [12, 13], etc appear as natural generalization of Einstein’s gravity. The Einstein Gauss Bonnet dilatonic (referred as DEGB) coupled interaction arises logically as the leading order in the low energy effective Heterotic string theory [10, 11]. As a consequence this interaction works satisfactory to explain inflation [14], as well as late-time acceleration [15] and is used also to study possible resolution of initial singularity [16, 17]. The singularity problem is still illusive, whose resolution has not yet become visible. The Euclidean wormhole [18, 19] is fascinating to alleviate initial cosmic singularity problem as well as to render a viable mechanism of vanishing of cosmological constant. A wormhole represents tunneling of a universe to another one through the classical singularity or equivalently a wormhole has two asymptotic regions connected by a tube with a minimum radius.

In the early nineties Coleman [20], Baum [21] and Hawking [22] proposed a mechanism of vanishing of cosmological constant in quantum cosmology introducing an idea of wormhole at the Planck era. Interestingly, Giddings and Strominger [23] first proposed the idea of wormhole from a solution of Euclidean field equations in the Einstein’s gravity with axionic field. In continuation several wormhole solutions [24–29] have been explored with different fields, as well as to study consequences of wormhole dynamics [20], [30–36]. The wormhole solution demands violation of null energy condition ($\rho_{eff} + p_{eff}$) ≥ 0 (NEC) [37], whose effect can be minimised by invoking some geometric contribution instead of exotic fields in the alternative theories of gravity [7–13]. The effective density and effective pressure are respectively ρ_{eff} and p_{eff} .

Cosmic evolution from the Planck era to the inflationary era is not smooth as the pre-inflationary era is governed by quantum gravity in curved spacetime [38, 39], while inflationary era can be described

*E-mail: biswasgb@gmail.com

[†]E-mail:mkdbrsnc@gmail.com

[‡]E-mail: bijanmodak@yahoo.co.in

by the field theory. Further it is thought that the spacetime is Euclidean in the early era, wherein the Euclidean time τ plays the role of time, while the GUT onward era is Lorentzian and the time t is the cosmic time. The Euclidean domain is classically forbidden in general and one cannot probe it with t , thus using Wick rotation $\tau = it$ one can analytically continue a function from one region to another or vice versa. Intuitively, the wormhole, if it exists at all in the Planck era, then subsequent cosmic evolution should yield an era of inflation at GUT era. Lorentzian wormholes have been studied in the DEGB theory [40–42], however viability of an inflation from a wormhole configuration has not been confirmed. In recent works [43–45] transition from wormhole configuration to inflationary era is evident by using $\tau = it$. A transition from wormhole solution to inflation is confirmed in [43] with numerical solutions in the DEGB theory with a few power law potentials. So we extend our earlier work of wormhole leading to inflation with exponential and inverse power law potentials [46] in the DEGB theory. In this extension, wormhole of multiple maxima and minima about the global minimum emerges in the Euclidean space with the inverse power law potential.

We consider both the analytic and numerical solutions of wormhole in the DEGB theory in 4-dimensional Robertson Walker Euclidean background. Analytic solutions are obtained with a simplifying assumption on the dynamical coupling $\Lambda(\phi)$ and with some constraints on the potential $V(\phi)$. Analytic solutions show wormhole configuration in the early era of τ . In some of the solutions we get a transition to an exponential era with time t after passing through an era of oscillating Euclidean universe.

The numerical wormhole solutions are considered with a few potentials favourable for inflation [46–48]. These solutions are presented with a plot of $a(\tau)$ as a function of Euclidean time τ , which show that two asymptotic domains are connected by a tube of finite radius at the minimum. The solution shows multiple maxima and minima about the global minimum for inverse power law potentials. The scale factor $a(\tau)$, overall increases with $|\tau|$ superimposed with tiny oscillation for inverse potentials. Now to explore the cosmic scenario of the numerical solutions we consider curve fit of $a(\tau)$ as polynomial of τ and consequently $a(t)$ is obtained by using $\tau = it$. The scale factor $a(t)$ is subsequently used to find the observable, namely the Hubble parameter $H(t)$ and the deceleration parameter $q(t)$. These are then used to investigate dynamical scenario of the wormhole and study cosmic evolution from a plot of $H(t)$ and $q(t)$ with cosmic time t .

Evolution of $H(t)$ and $q(t)$ from these plots show an initial collapsing era up to $t = t_i$ before encountering some unusual feature (not familiar in classical regime) around the throat of the wormhole followed by final expansion beginning at $t = t_f$. The domain $(t_f - t_i)$ seems to be the classical forbidden regime of the wormhole. The parameter $H(t)$ approaches to a constant value at $t \gg t_f$, simultaneously $q(t) \rightarrow -1$. Thus a phase transition from an Euclidean space to Hyperbolic (Lorentzian) space through the Wick rotation $\tau = it$ yields the evolution from a wormhole configuration to an inflationary era far away from the throat of the wormhole [49–51]. The evolution agrees well with the classical scenario far away from the throat of the wormhole. The potential of the dilaton field decreases to a very small value at large time τ . The NEC is satisfied in all analytic and numerical solutions in the neighbourhood of the throat, while in the numerical solution it is also satisfied far away from the throat.

We present the field equations in section 2. In section 3 analytic solutions are considered. Numerical solutions of the field equations are presented in section 4. We interpret the numerical solutions in section 5. Section 6 contains a brief discussion and finally an Appendix is given in section 7.

2 Action with Einstein Gauss-Bonnet dilaton interaction and the field equations:

We consider the action as

$$S = \int d^4x \sqrt{g} \left[\frac{R}{2K^2} - \frac{\gamma}{2} \phi_{;\mu} \phi^{;\mu} - V(\phi) - \frac{\Lambda(\phi)}{8} \mathcal{G} \right] + S_m, \quad (1)$$

where S_m is the surface term, K is the inverse of Planck mass, γ is a constant and the Gauss-Bonnet curvature is $\mathcal{G} = R_{\mu\nu\alpha\beta} R^{\mu\nu\alpha\beta} - 4R_{\mu\nu} R^{\mu\nu} + R^2$. Further $\Lambda(\phi)$ is the coupling of the GB term with the dilatonic field ϕ [48, 52] and $V(\phi)$ is the potential of the field ϕ . R is the Ricci scalar. In Robertson Walker Euclidean metric

$$ds^2 = d\tau^2 + a^2(\tau) \left[\frac{dr^2}{1 - \kappa r^2} + r^2(d\theta^2 + \sin^2 \theta d\phi^2) \right],$$

the field equations from (1) are

$$\frac{3}{K^2} \left(\frac{a'^2}{a^2} - \frac{\kappa}{a^2} \right) = \frac{\gamma}{2} \phi'^2 - V(\phi) - 3\Lambda' \frac{a'}{a} \left(\frac{a'^2}{a^2} - \frac{\kappa}{a^2} \right), \quad (2)$$

$$-\frac{1}{K^2} \left(2\frac{a''}{a} + \frac{a'^2}{a^2} - \frac{\kappa}{a^2} \right) = \frac{\gamma}{2} \phi'^2 + V(\phi) + \Lambda'' \left(\frac{a'^2}{a^2} - \frac{\kappa}{a^2} \right) + 2\Lambda' \frac{a'' a'}{a^2} \quad (3)$$

and

$$\gamma \left(\phi'' + 3\frac{a'}{a} \phi' \right) = V_{,\phi} + 3\Lambda_{,\phi} \frac{a''}{a} \left(\frac{a'^2}{a^2} - \frac{\kappa}{a^2} \right) = \frac{\partial V_{eff}}{\partial \phi}, \quad (4)$$

where $a(\tau)$ is the scale factor, V_{eff} is the effective potential and $\frac{\partial V_{eff}}{\partial \phi}$ is the effective potential gradient having contribution from the potential $V(\phi)$ and dilaton coupling $\Lambda(\phi)$. Here, κ is the 3-space curvature parameter ($\kappa = 0, \pm 1$). A prime denotes derivative with respect to Euclidean time τ , whereas a comma $(,)$ denotes partial derivative. Evolution of the universe is determined by the equations (2)-(4) with a given dilaton coupling $\Lambda(\phi)$ and potential $V(\phi)$.

A wormhole should satisfy following conditions to be a solution of the field equations. A wormhole has two asymptotic regions connected by a tube with a non-vanishing minimum of the scale factor $a(\tau)$ at the throat at $\tau = \tau_0$, where $a'(\tau_0) = 0$, $a''(\tau_0) > 0$, further $a(\tau) \neq 0$, $a'' \leq 0$ at other τ . Then the field equation (2) at $\tau = \tau_0$ yields

$$\frac{3}{K^2} \frac{\kappa}{a_0^2} = -\frac{\gamma}{2} \phi_0'^2 + V_0, \quad (5)$$

where a subscript “0” on a variable denotes the value of the variable at τ_0 . So from (5) it is clear that the potential energy V_0 at the throat is very large positive as a_0 is small therein with $\kappa = 1$. Again from (3) and (5), $a''(\tau)$ at the extrema is

$$a_0'' = \frac{K^2}{3} (-\gamma \phi_0'^2 - V_0) a_0 + \frac{\kappa K^2 \Lambda_0''}{2 a_0}. \quad (6)$$

The Gauss-Bonnet term is assumed to be a small correction to the gravity, however the term $\frac{\Lambda_0''}{a_0}$ in (6) may be large and it may take both positive and negative value; so the scale factor may have multiple maxima and minima. Thus to ensure lower bound of $a(\tau)$ one should satisfy $\phi_0'^2 > V_0$ for $\gamma = -1$ and $\kappa = 1$ assuming $\frac{\Lambda_0''}{a_0} > 0$ and $V_0 > 0$. On the other hand, we may have local maxima or minima of $a(\tau)$ depending on the magnitude and the sign of $\frac{\Lambda_0''}{a_0}$ and V_0 at the corresponding local extrema. Analytic solution is quite non-trivial in general with specific $V(\phi)$ and $\Lambda(\phi)$ for $\kappa \neq 0$. So we present a few analytic solutions with simplifying assumption for $\kappa = 0$ in the next section.

3 Analytic solution of the field equations for wormhole configuration:

Analytic solution is quite non trivial, so we consider assumption to get a glimpse of evolution in the very early universe. The solution of the field equations requires knowledge of $\Lambda(\phi)$ and $V(\phi)$. We simplify the field equations with a restriction on the coupling function $\Lambda(\phi)$ as

$$\Lambda' \frac{a'}{a} = \frac{2m}{K^2}, \quad (7)$$

where m is a constant. In some earlier works [53, 54] the condition (7) has been used to study late time acceleration in the DEGB theory. Now using (7) in combination of (2) and (3) for $\kappa = 0$ we get

$$-2(m+1)a''a + (4m+2)a'^2 = \gamma \phi'^2 a^2 K^2 \quad \text{and} \quad (8)$$

$$(m+1)a''a + (4m+2)a'^2 = -V(\phi)a^2 K^2. \quad (9)$$

Now from (8) and (9) the condition of non-vanishing minimum radius of the wormhole, i.e. $a'_0 = 0$ and $a''_0 > 0$ at the throat at some time τ_0 can be satisfied assuming $\gamma = -1$ for $m+1 > 0$ with real scalar field, but with $V(\phi_0) < 0$ at the throat, which yields the conditions $\frac{a_0''}{a_0} = \frac{K^2 \phi_0'^2}{2(m+1)}$ and $\frac{a_0''}{a_0} = -\frac{K^2 V(\phi_0)}{m+1}$. The form of (8) and (9) are simple for solution with a knowledge of $V(\phi)$. Now we consider a few solutions with choice of $V(\phi)$.

3.1 Solution with vanishing effective potential gradient:

The contribution of Gauss Bonnet coupling term in the field equations gives rise to an additional potential apart from $V(\phi)$. The term in the right side of (4) is an effective potential gradient and the dilaton field evolved under influence of this potential gradient. Instead of considering form of $V(\phi)$ we simplify the field equations assuming that the dilaton field is free from the influence of effective potential gradient, then (4) for $\kappa = 0$ leads to

$$\phi' a^3 = c_0, \quad \text{and} \quad V' = -3\Lambda' \frac{a'' a'^2}{a^3}, \quad (10)$$

from which we can determine the potential, where c_0 is a constant. Now using above ϕ' with $\Lambda' \frac{a'}{a} = \frac{2m}{K^2}$ and $\gamma = -1$ in (8) we have

$$(m+1) \frac{a''}{a} - (2m+1) \frac{a'^2}{a^2} = \frac{K^2 \phi'^2}{2} = \frac{K^2 c_0^2}{2a^6}. \quad (11)$$

The first integral of (11) gives

$$a^4 a'^2 = -\frac{K^2 c_0^2}{8m+6} + r_0^2 a^{\frac{8m+6}{m+1}}, \quad (12)$$

where r_0 is a constant, so we have a lot of solutions with different values of m . Now for a wormhole solution $a' = 0$ at the throat at some τ , wherein $a_0'' > 0$. So at the throat

$$a_0^{\frac{8m+6}{m+1}} = \frac{K^2 c_0^2}{(8m+6)r_0^2} \quad \text{and} \quad a_0'' = \frac{K^2 c_0^2}{2(m+1)a_0^5}, \quad (13)$$

so for wormhole solution both $(4m+3) > 0$ and $(m+1) > 0$. The null energy condition can be obtained from the field equations (2) and (3) using (12) considering sum of the effective energy density and effective pressure as

$$\rho_{eff} + p_{eff} = \frac{2mr_0^2}{(m+1)K^2} a^{\frac{2m}{m+1}} + \frac{6c_0^2}{(8m+6)a^6}, \quad (14)$$

which shows that the energy condition may be satisfied near the throat with restricted value of m . To get an explicit evolution with τ we choose the value of m .

3.1.1 Evolution of the universe for $m = -\frac{2}{3}$:

A simple choice of m yields solution of (11) as

$$\frac{a}{2} \sqrt{a^2 - a_0^2} + \frac{a_0^2}{2} \log \left[a + \sqrt{a^2 - a_0^2} \right] = \pm r_0 \tau + r_1, \quad (15)$$

where, $m = -\frac{2}{3}$ and r_1 is an integration constant. Further r_1 can be determined using the idea that the radius of throat $a = a_0$ occurs at $\tau = 0$, so $r_1 = \frac{a_0^2}{2} \log[a_0]$, where $a_0 = \sqrt{\frac{3}{2} \frac{Kc_0}{r_0}}$. The solution (15) is a wormhole solution. Near the throat (i.e. $a \sim a_0$) second term in left side of (15) is dominating, then (15) gives

$$a(\tau) = a_0 \cosh(\omega\tau) \quad \text{at} \quad a \sim a_0, \quad \text{while at} \quad a \gg a_0, \quad a^2 = \frac{a_0^2}{2} + \sqrt{\frac{a_0^4}{4} + (r_0\tau + r_1)^2}, \quad (16)$$

where $\omega = \frac{2r_0}{a_0^2}$. The expression $a(\tau) = a_0 \cosh(\omega\tau)$ confirms Euclidean wormhole in the early era.

It is interesting to note that $\frac{a'}{a} = \frac{1}{2\tau}$ at large τ or when $r_0\tau \gg r_1$ as well as $r_0\tau \gg a_0$. So, under analytic continuation $\tau = it$, we get $\frac{\dot{a}}{a} = \frac{1}{2t}$, which corresponds to standard form of expansion for radiation dominated era. Thus an initial wormhole configuration evolves to a radiation dominated era asymptotically. The potential $V(\phi)$ in this case leads to

$$V(a) = \frac{c_0^2}{a^6} \left[\frac{3}{2} \frac{a^2}{a_0^2} - 2 \right]. \quad (17)$$

The potential $V(a)$ is positive at $a(\tau) > \frac{2a_0}{\sqrt{3}}$ and negative for $a(\tau) < \frac{2a_0}{\sqrt{3}}$. Further (14) now reduces to

$$\rho_{eff} + p_{eff} = \frac{4r_0^2}{K^2 a^6} \left(\frac{3a_0^2}{2} - a^2 \right). \quad (18)$$

Thus NEC is satisfied near the throat as long as $a(\tau) < \sqrt{\frac{3}{2}} a_0$

3.2 Solution with a choice of potential of the dilaton field:

The solution of the field equation with standard form of potential is non-trivial, so we assume potential V as a function of the scale factor $a(\tau)$ [55] in the form

$$V(\phi(\tau)) = \frac{v_0}{a^\alpha} - u_0. \quad (19)$$

The choice of potential seems artificial, however it is possible when the background spatial section is homogeneous, where u_0 , v_0 and α are constants. Now introducing (19) in (9) and with an integration we get

$$a'^2 = -\frac{2v_0K^2 a^{2-\alpha}}{[10m+6-\alpha(m+1)]} + \frac{2u_0K^2a^2}{10m+6} + c_2a^{-4\frac{(2m+1)}{(m+1)}}, \quad (20)$$

where c_2 is an integration constant. Now we have the following class of solutions depending on m , v_0 , u_0 , α and c_2 .

3.2.1 Solution for $\alpha = 4$, $m = -\frac{1}{2}$, but $c_2 \neq 0$:

The equation (20) with a simple choice of $\alpha = 4$, $m = -\frac{1}{2}$ and $c_2 \neq 0$ reduces to

$$\left(\frac{da}{d\hat{\tau}}\right)^2 = 1 + h_0^2 a^2(\hat{\tau}) - \frac{H_0^2}{a^2(\hat{\tau})}, \quad (21)$$

where $\hat{\tau} = \sqrt{c_2}\tau$, $h_0^2 = \frac{2u_0K^2}{c_2}$ and $H_0^2 = -\frac{2v_0K^2}{c_2}$. In a separate work [56] on R^2 gravity similar equation (21) appeared in discussion of wormhole. It is to note that $\frac{H_0^2}{a^2(\hat{\tau})}$ term in (21) is dominating in the early era of evolution, while $h_0^2 a^2(\hat{\tau})$ has a large contribution in the later epoch. So the different terms in (21) lead to distinct cosmic evolution and the evolution also depend on the signature of these terms. Accordingly we consider the following piece-wise solutions which are relevant to the different domains of $a(\hat{\tau})$ according to greater contribution of individual terms in the right side of (21). Further from the field equations (2) and (3) using (21) we can determine the NEC as

$$\rho_{eff} + p_{eff} = \frac{2c_2}{K^2 a^4} (2H_0^2 - a^2), \quad (22)$$

so the NEC will be satisfied near the throat as long as $a < \sqrt{2}H_0$ and it is violated for $a > \sqrt{2}H_0$.

3.2.2A: Evolution when $h_0^2 a^2(\hat{\tau}) \ll \frac{H_0^2}{a^2(\hat{\tau})}$ in the early universe:

In the very early era near to the classical singularity contribution of $h_0^2 a^2(\hat{\tau})$ is very small compared to $\frac{H_0^2}{a^2(\hat{\tau})}$; so in the early era we can neglect the contribution of $h_0^2 a^2(\hat{\tau})$. Thus (21) in the early era gives

$$a^2(\hat{\tau}) = H_0^2 + \hat{\tau}^2 \quad (23)$$

apart from an integration constant. The equation (23) represents a wormhole solution and the radius at the throat is H_0 . The scale factor is symmetric and increases with $\hat{\tau}$. So, from (22) the NEC is not violated as long as $\tau < H_0$. The dilaton field from (8) and (23) gives

$$K\phi = \pm \tan^{-1}\left(\frac{\hat{\tau}}{H_0}\right) \quad (24)$$

apart from a constant, which shows that $\phi = 0$ at $\hat{\tau} = 0$ and ϕ is real.

Further at sufficiently large scale factor the contribution of $h_0^2 a^2(\hat{\tau})$ in (21) also influences evolution, so we consider contribution of all terms in (21) in next subsection.

3.2.2B: Evolution when $h_0^2 a^2(\hat{\tau})$ is not negligible with $\frac{H_0^2}{a^2(\hat{\tau})}$ at some intermediate era:

The solution of (21) in above regime is

$$a^2(\hat{\tau}) = \frac{1}{2h_0^2} [-1 + r_5 \cosh(2h_0\hat{\tau})], \quad (25)$$

where r_5 is constant and $r_5^2 = 1 + 4h_0^2 H_0^2$ assuming the condition $a'(\hat{\tau} = 0) = 0$ at the throat. The solution (25) represents a wormhole as $r_5 > 1$ assuming h_0^2 and H_0^2 are positive. The scale factor $a(\hat{\tau})$ increases exponentially at large $\hat{\tau}$ at $2h_0\hat{\tau} \gg 1$. However, in the early era (25) gives $a^2(\hat{\tau}) \sim \frac{r_5-1}{2h_0^2} + r_5\hat{\tau}^2$ in the domain $2h_0\hat{\tau} \ll 1$ taking lowest order contribution in the early era. This also agrees with (23) with a redefined $\hat{\tau}$.

3.2.2C: Evolution when $h_0^2 a^2(\hat{\tau})$ is not negligible with $\frac{H_0^2}{a^2(\hat{\tau})}$ at some intermediate era, but $h_0^2 = -h_1^2 < 0$ and $4h_1^2 H_0^2 < 1$:

In above condition on $a(\hat{\tau})$ and $h_0^2 < 0$ the solution of (21) is

$$a^2(\hat{\tau}) = \frac{1}{2h_1^2} \left[1 + (1 - 4h_1^2 H_0^2)^{\frac{1}{2}} \sin(2h_1 \hat{\tau}) \right], \text{ in the domain } a^2(\hat{\tau}) < a_0^2, \quad (26)$$

apart from an integration constant, where $a_0^2 = \frac{1}{2h_1^2} \left[1 + (1 - 4h_1^2 H_0^2)^{\frac{1}{2}} \right]$. So, we have oscillation of the scale factor in Euclidean time. Again at $a^2(\hat{\tau}) > a_0^2$, the scale factor $a(\hat{\tau})$ evolves as

$$a^2(\hat{\tau}) = \frac{1}{2h_1^2} \left[1 + (1 - 4h_1^2 H_0^2)^{\frac{1}{2}} \cos(2h_1 \hat{\tau}) \right], \quad (27)$$

The equation (27) also gives the oscillation of the scale factor in Euclidean time. Now with analytic continuation with $\tau = it$ (27) gives $a^2(\hat{t}) = \frac{1}{2h_1^2} \left[1 + (1 - 4h_1^2 H_0^2)^{\frac{1}{2}} \cosh(2h_1 \hat{t}) \right]$, which is a wormhole configuration with t and asymptotically evolves exponentially.

3.2.2D: Evolution when $h_0^2 a^2(\hat{\tau}) \gg \frac{H_0^2}{a^2(\hat{\tau})}$ at late era with $h_0^2 = -h_1^2 < 0$:

In the later era $\frac{H_0^2}{a^2(\hat{\tau})}$ is negligible with the term $h_0^2 a^2(\hat{\tau})$ in (21), so assuming $\frac{H_0^2}{a^2(\hat{\tau})} \approx 0$ the scale factor at $a(\hat{\tau})h_1 > 1$ evolves as

$$a^2(\hat{\tau}) = \frac{1}{h_1^2} \cos^2(h_1 \hat{\tau}), \text{ so with } \tau = it, \quad a(\hat{t}) = \frac{1}{h_1} \cosh(h_1 \hat{t}), \quad (28)$$

apart from an integration constant. This gives an expanding universe with cosmic time t (where $\hat{t} = \sqrt{c_2} t$) and asymptotically at $h_1 \hat{t} \gg 1$, the expansion is exponential. Now the dilaton field from (28) and (8) gives

$$iK \phi = \pm h_1 \hat{\tau} \quad (29)$$

apart from an integration constant. So the scalar field ϕ is imaginary with respect to τ .

Now one can interpret the cosmic scenario of (28) as the solutions of an oscillating universe in the Euclidean time before crossing the deSitter radius $\frac{1}{h_1}$ and eventually the universe expands exponentially with proper time t after crossing the deSitter radius.

We have piece-wise solutions of (21) as (23), (25), (27) and (28) according to dominating contribution of different terms in the right side of (21). In a nutshell we can interpret and unify these piece-wise solutions representing cosmic scenario of an universe beginning from the solution (23) in the very early era and subsequent evolution passes through era described by (25) and (27). In solution (27) the universe oscillates with $\hat{\tau}$ after passing an expansion through (25) in $\hat{\tau}$. Finally the universe emerges to an expanding era (with cosmic time \hat{t} given by (28)) after crossing the radius $\frac{1}{h_1}$ of an oscillating universe. Asymptotically we can achieve exponential expansion.

Now we consider numerical solutions of the field equations with a few standard potentials with $\kappa = 1$ and $\gamma = -1$ to get wormhole configuration

4 Numerical solution of the Euclidean field equations with $V(\phi)$ and dilaton coupling $\Lambda(\phi)$:

Now we consider numerical solution of the field equations to study wormhole configuration assuming $\Lambda(\phi)$ and $V(\phi)$. Analytical solution of the field equations in general is quite non-trivial, so we consider numerical solution for $\kappa = 1$ case. Let us choose dilaton coupling $\Lambda(\phi) = \Lambda_0 e^{-\nu\phi}$ [57] in solving the field equations, where Λ_0 and ν are constants. The numerical solution of (2), (3) and (4) gives us wormhole solutions with exponential and inverse power law potentials. We present these numerical solutions graphically using initial conditions on $(a(\tau), a'(\tau), \phi(\tau), \phi'(\tau))$. They yield two distinct categories of wormhole depending on the potential. In one category we have usual model of wormhole of single lower bound, while in other models we have wormhole with multiple minima and maxima around a global minimum. The potential decays asymptotically with decaying amplitude in all cases.

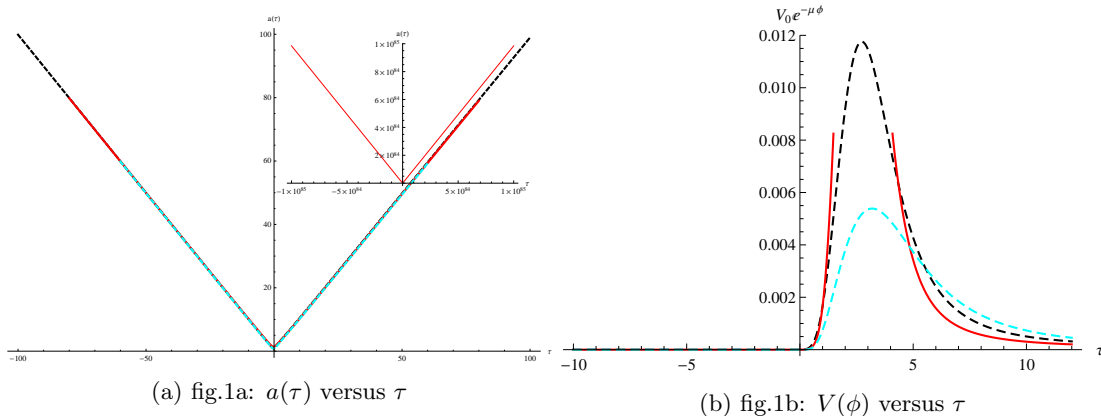


Figure 1: The evolution of $a(\tau)$ and $V(\phi)$ with τ are shown respectively in fig.1a and fig.1b for $e^{-\mu\phi}$ potential with $\gamma = -1$, $V_0 = 1$, $K = 1$, $\kappa = 1$, $\nu = 1$, $\mu = 8$ and $\Lambda_0 = 1$. The initial conditions on $(a(\tau), a'(\tau), \phi(\tau), \phi'(\tau))$ for the solution along the black dashed, red and cyan dashed curves are respectively $(1.9, 0.9, 0.8, -0.4)$, $(2, 0.8, 0.8, -0.55)$ and $(1.6, 0.9, 0.9, -0.4)$ at $\tau = 1$.

4.1 Solution with exponential potential $V_0 e^{-\mu\phi}$ and inverse power law potential $V_0 \phi^{-\alpha}$ for $\alpha = 2, 1, \frac{1}{2}$, etc. :

The numerical solution of the Euclidean field equations with potential $V(\phi)$ for a field [58] yields evolution of the universe with Euclidean time τ . The numerical solution gives evolution of the scale factor $a(\tau)$ and the dilaton field $\phi(\tau)$ graphically as a function of τ . The evolution of the scale factor and corresponding potential are shown respectively in fig.1a and fig.1b for $V_0 e^{-\mu\phi}$ potential. Further the scale factors and the corresponding potentials are given respectively in fig.2a and fig.2b for inverse potential $V_0 \phi^{-\alpha}$ [46] for $\alpha = 2, 1, \frac{3}{2}$, etc. The fig.2a is a superposition of plot of $a(\tau)$ with τ for $V_0 \phi^{-2}$, $V_0 \phi^{-1}$ and $V_0 \phi^{-\frac{3}{2}}$ potentials considering three initial conditions for each of them. The scale factor $a(\tau)$ is non-vanishing with a lower bound in each solution. In fig.1a, $a(\tau)$ increases with $|\tau|$ without any oscillations and $a(\tau)$ shows a single minimum for exponential potential, while in fig.2a there is an oscillations of $a(\tau)$ with τ . In fig.2a, $a(\tau)$ shows an overall ascending nature with increasing $|\tau|$ accompanying with multiple non-vanishing minima and finite maxima around a global non-vanishing minimum. The fluctuations of $a(\tau)$ with τ in fig.2a continues even for large τ . The plot of $a(\tau)$ versus τ is almost symmetric about the global minimum (or single minimum) in each solution. The scale factor $a(\tau)$ is finite with τ in all cases. So the solution of $a(\tau)$ versus τ represents wormhole configuration.

The variation of potential $V(\phi)$ with τ are shown in fig.1b and fig.2b respectively for $V_0 e^{-\mu\phi}$ and $V_0 \phi^{-\alpha}$ potentials. In all cases, the potential $V(\phi)$ is maximum near the throat of the wormhole and decays sharply without any oscillations from its maximum on both sides about this peak and asymptotically decays significantly to very small, but finite value even at large τ . The interpretation of above solutions are considered later on after presenting some other solutions with inverse power law potentials.

Above characteristics of $a(\tau)$ with τ in fig.2a are almost identical with other inverse power law potential with $\alpha = 2.6, \frac{5}{2}, \frac{7}{3}, \frac{5}{3}$, etc. The variation of $V(\phi)$ with τ are also identical for other power law potentials. Numerical solutions (see Appendix-I) of them are obtained using same initial condition for each α , which are given in fig.6a and fig.6b respectively. An interesting feature is that expansion rate of $a(\tau)$ is greater for larger α .

5 Cosmic scenario of the early universe from curve fit of the numerical solution:

Now we consider dynamical consequence of the wormhole solutions, and hence functional form of the scale factor is necessary to study cosmic evolution of the early universe. So, we consider curve fitting of the numerical solution of $a(\tau)$ close to the throat of wormhole for $V_0 \phi^{-2}$ potential. We also consider curve fitting for exponential potential (given in Appendix III). Hubble expansion $H(t)$ and deceleration parameter $q(t)$ are the relevant parameters at first-hand to determine cosmic evolution and we can evaluate them by using expression of $a(t)$ obtained by fit of $a(\tau)$ and with analytic continuation $\tau = it$. The evolution of $H(t)$ and $q(t)$ are almost independent of potentials. The plot of H and q as a function

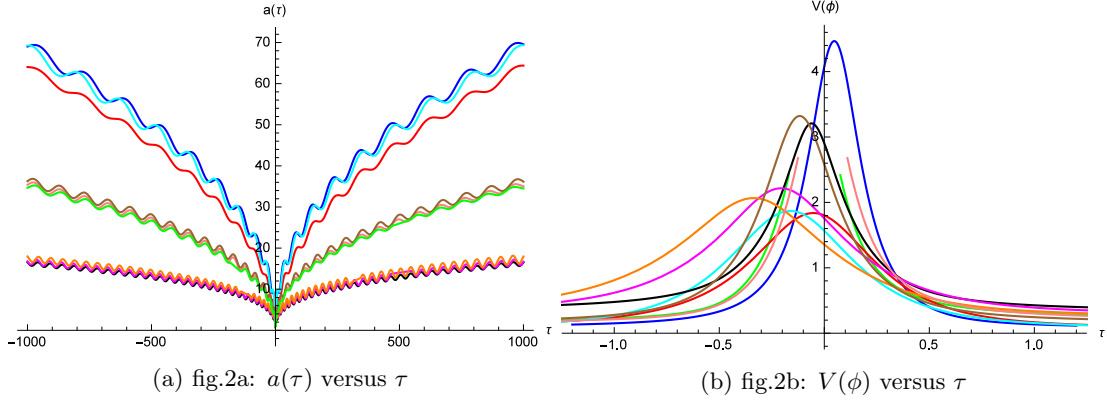


Figure 2: The evolution of $a(\tau)$ and $V(\phi)$ with τ are shown respectively in fig.2a and fig.2b for inverse potential with $\gamma = -1$, $V_0 = 1$, $K = 1$, $\kappa = 1$, $\nu = 0.7$ and $\Lambda_0 = 1$. Three sets of initial conditions are chosen on $(a(\tau), a'(\tau), \phi(\tau), \phi'(\tau))$ at $\tau = 0.1$ for each potential. The initial conditions on blue, red and cyan curves are respectively $(2, -0.512559, .5, 1)$, $(1.6, -0.4, 0.8, .8)$ and $(2.5, -0.5, 0.9, 1.2)$ for ϕ^{-2} potential. The initial conditions on brown, green and pink curves are respectively $(1.5, -0.4, 0.7, 2)$, $(1, -0.3, 0.61, 2.4)$ and $(1.2, -0.2, 0.5, 1.8)$ for $\phi^{-\frac{3}{2}}$ potential, while black, magenta and orange curves are drawn with initial conditions $(1, -0.5, 0.5, 2)$, $(1.4, -0.5, 0.7, 1.5)$ and $(1.6, -0.7, 0.9, 1.8)$ for ϕ^{-1} potential.

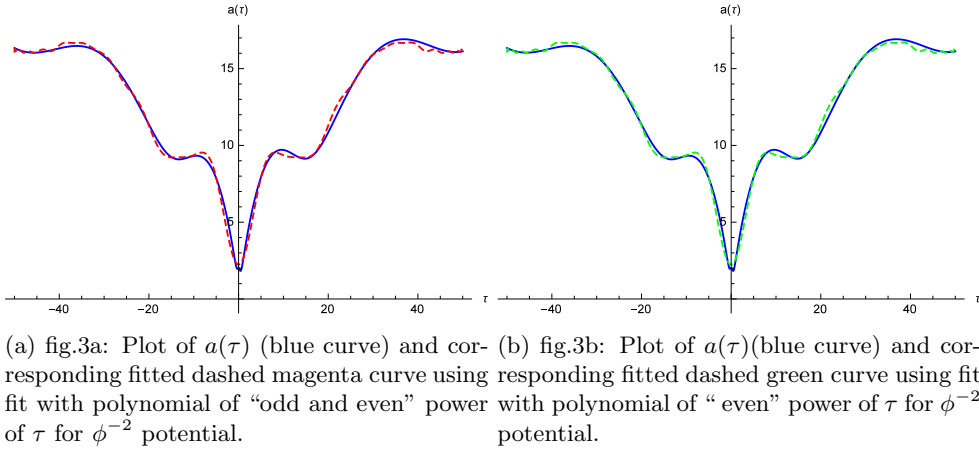


Figure 3: The initial conditions in numerical solution of $a(\tau)$ shown in blue curve of fig.3a and fig.3b are $(a(0.1) = 2, a'(0.1) = -0.5125559, \phi(0.1) = 0.5, \phi'(0.1) = 1)$ with $\gamma = -1$, $V_0 = 1$, $K = 1$, $\kappa = 1$, $\nu = 0.7$ and $\Lambda_0 = 1$.

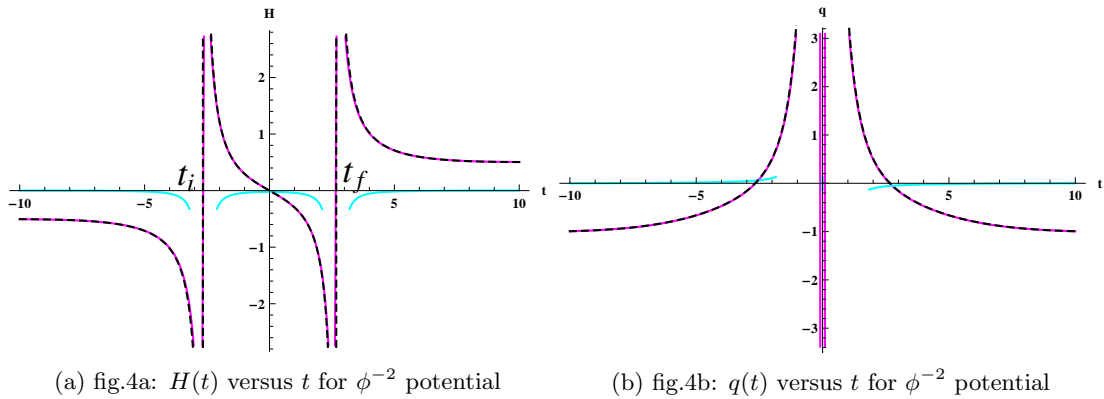


Figure 4: The evolution of $H(t)$ and $q(t)$ with t are shown respectively in fig.4a and fig.4b. Real and imaginary parts of $H(t)$ and $q(t)$ obtained from the fit of $a(\tau)$ with polynomial of "odd and even" power of τ are shown respectively in magenta and cyan curves. Again fit of $a(\tau)$ with polynomial of "even" power of τ leads to real $H(t)$ and $q(t)$, which are shown by dashed curves.

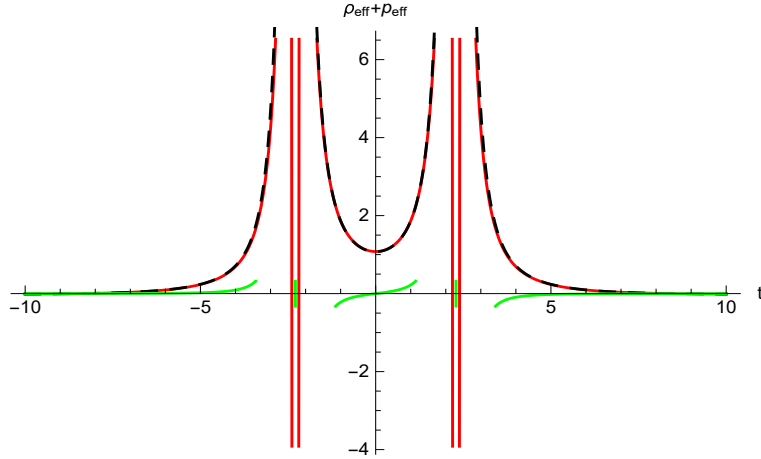


Figure 5: The evolution of $\rho_{eff} + p_{eff}$ with t for ϕ^{-2} potential. The red and green curves are shown respectively for real and imaginary parts of $\rho_{eff} + p_{eff}$ using fit of $a(\tau)$ by polynomial of odd and even power of τ given in (34), while black curve is obtained by fit of $a(\tau)$ using polynomial of even power of τ given in (35).

of t yield cosmic evolution from above fitting. Two distinct expressions of $a(\tau)$ may appear depending on the curve fitting in each wormhole which are given in the following section.

5.1 Cosmic evolution near the throat of wormhole by curve fit of $a(\tau)$ with a polynomial of τ for $V_0\phi^{-2}$ potentials:

We consider curve fitting of the numerical solution of $a(\tau)$ within a small domain about the throat of wormhole. Two distinct expressions of $a(\tau)$ may appear depending on the fit either with a polynomial of “odd and even” power of τ , or with a polynomial of “even” power of τ in each numerical solution. The fitted curves are shown in fig.3a and fig.3b respectively for polynomial of “odd and even” and “even” power of τ for $V_0\phi^{-2}$ potential. The expression of $a(\tau)$ using polynomial of “odd and even” power of τ reads as

$$a(\tau) = \sum_{n=0}^N b_n \tau^n, \quad (30)$$

while for polynomial of “even” power of τ is

$$a(\tau) = \sum_{n=0}^M c_{2n} \tau^{2n}, \quad (31)$$

where b_n and c_{2n} are the coefficients in the polynomials, and they depend on the potential and initial conditions. The explicit expression of (30) and (31) for the potential $V_0\phi^{-2}$ are given respectively in (34) and (35) in the Appendix-II. We assume the functions $1, \tau, \tau^2, \tau^3, \tau^4, \dots$ with $N = 50$ in (30) for ϕ^{-2} potential in the curve fit of numerical solution. Further we choose $M = 25$ in the fit with even power of τ in equation (31). The fitted curves are shown in fig.7a and fig.7b respectively for polynomial of “odd and even” and “even” power of τ for $V_0e^{-\mu\phi}$ potential. Again the expression of (30) and (31) for $V_0e^{-\mu\phi}$ potential are given respectively in (36) and (37) in the Appendix-III.

The fit with only even or odd powers of τ does not reveal good fit, however a fit with $1, \tau, \tau^2, \tau^3, \tau^4, \dots$ yields a better one. On the basis of the fit the metric tensor in Euclidean space $g_{ik} \propto a^2(\tau)\delta_{ik}$ are determined as a function of τ and $g_{00} = 1$; where i, k runs $1, 2, 3$. Analytic continuation in the Euclidean space by the Wick rotation $\tau = it$ leads the metric tensor in terms of time t . However, the resulting spacetime seems to be different from a Lorentz spacetime due to presence of real and imaginary parts of $a(t)$. The presence of odd power of τ in the fit gives rise imaginary parts of $a(t)$ and the parameters dependent on $a(t)$ also yield real and imaginary parts. This feature is not surprising, since quantum mechanical process is dominant near the throat. In fact a wormhole configuration in general comprised of classical forbidden domain ($t_i \leq t \leq t_f$) surrounded by a classical allowed region ($t < t_i$ and $t > t_f$, where t_i and t_f are given in the next section). The coordinate “ t ” in the classical allowed domain is the usual time, while “ t ” in the classical forbidden domain changes its usual notion of cosmic time, and the dynamical variables may give rise both real and imaginary parts inside the classical forbidden domain.

However, a fit with polynomial of “even” power of τ does not yield any imaginary parts either in $a(t)$, or in other variables. So we can alleviate the imaginary parts using a fit of even power of τ .

5.2 Evolution of observable parameters $H(t)$ and $q(t)$ from the fit and interpretation:

The observable quantities $H(t) = \frac{\dot{a}}{a}$ and $q(t) = -\frac{a\ddot{a}}{\dot{a}^2}$ are evaluated both from (34) and (35), where an overhead dot is derivative with t . The plot of $H(t)$ and $q(t)$ are shown respectively in fig.4a and fig.4b for ϕ^{-2} potential, while for $e^{-\mu\phi}$ potential, $H(t)$ and $q(t)$ are shown respectively in fig.8a and fig.8b. The evolution of $H(t)$ and $q(t)$ in above solution are distinct from the usual real value of them in the cosmic evolution. However in recent work [44], we have obtained similar evolution of $H(t)$ both from analytic and numerical solutions but with a different action.

The parameters $H(t)$ and $q(t)$ have both real (shown by magenta curves) and imaginary (drawn by cyan curves) parts close to the throat, when the numerical solution is fitted with polynomial of “odd and even” power of τ . Again, $H(t)$ and $q(t)$ obtained by using fit with polynomial of “even” power of τ yields real value (black dashed curves in fig.4a and fig.4b), which are identical with the respective real parts of $H(t)$ and $q(t)$ obtained with fit of “odd and even” power of τ . Real parts of them dominates over the imaginary parts away from the throat. Imaginary parts of them almost vanishes at large t , and asymptotically $H(t)$ approaches to a constant value and the deceleration parameter $q(t)$ simultaneously approaches to -1 away from the throat. Thus an inflationary era can be achieved from the wormhole solution by analytic continuation $\tau = it$ at time t away from the throat irrespective of the curve fit. The evolution of $H(t)$ and $q(t)$ for ϕ^{-2} potential are identical with those $H(t)$ and $q(t)$ for $e^{-\mu\phi}$ potential, except the value of t_i and t_f .

Null energy condition is obtained by finding $\rho_{eff} + p_{eff}$ from the field equations using solution (34) and (35) respectively for fit given in fig.3a and fig.3b. The plots of $\rho_{eff} + p_{eff}$ versus t are given in fig.5, which shows that the NEC is not violated in the neighbourhood of the throat. Further $\rho_{eff} + p_{eff}$ vanishes far away from the throat. Imaginary part of $\rho_{eff} + p_{eff}$ is very small with respect to its real part. The imaginary part appeared due to choice of fit of $a(\tau)$ with polynomial of both odd and even power of τ . The imaginary part can be removed using fit of $a(\tau)$ with polynomial of even power of τ and all the observables turned to be real.

It is interesting to note that the metric tensor g_{ik} or $a^2(t)$ from (30) or (31) vanishes at $t = t_i$ and $t = t_f$, where $t_i = -2.7$ and $t_f = +2.7$ for ϕ^{-2} potential. Further evolution of $H(t)$ in the domain $t < t_i$ is a collapsing mode, while the domain $t > t_f$ is an expanding era in fig.4a. In between above collapsing and expanding modes, an unusual evolution is evident in the domain $t_i \leq t \leq t_f$ surrounding the throat with respect to t , wherein $a(\tau)$ is well behaved with τ . In fact $t_i \leq t \leq t_f$ is the classical forbidden domain, while the domains $t < t_i$ and $t > t_f$ are classical allowed with respect to time t .

Imaginary parts of $H(t)$ and $q(t)$ obtained above are questionable from the observational ground, however, the imaginary part of the $H(t)$ may lead to a very small oscillation of the scale factor near the throat. Further the potential is maximum near the throat and the fall of potential is evident from the plot of $V(\phi)$ with τ .

The potential is decaying, but it is vanishingly small even at large τ . An estimate of decrease for $V_0 e^{-\mu\phi}$ potential yields $\frac{V(\tau=2.7)}{V(\tau=10^{30})} \approx 10^{63}$ and $\frac{V(\tau=2.7)}{V(\tau=10^{65})} \approx 10^{132}$ with initial condition given in black(dashed) curve of fig.1b. So inflationary expansion is a consequence of the wormhole solution in the Einstein Gauss-Bonnet scalar tensor theory.

5.3 Possibility of multiple minima and maxima in a wormhole with inverse potential:

The evolution of the scale factor $a(\tau)$ with τ for inverse potential shows multiple maxima and minima about the global minimum at the throat of wormhole. Interestingly, multiple maxima and minima in above plot of $a(\tau)$ are not reflected in cosmic evolution of Hubble parameter $H(t)$, rather they represent an average nature [59]. However, one may get clue from expression of $a''(\tau)$, since $a'' > 0$ at the minima, while at the maxima $a'' < 0$. Now from (2) and (3), we have

$$a''(\tau) = -b(\tau)a'(\tau) - \left(b'(\tau) + \omega_0^2(\tau)\right)a(\tau) \quad (32)$$

where $b(\tau) = \frac{K^2}{2}\Lambda'\left(\frac{a'^2}{a^2} - \frac{\kappa}{a^2}\right)$, $\omega_0^2(\tau) = \frac{K^2}{3}\left(\gamma\phi'^2 + V(\phi)\right)$. The evolution of $a(\tau)$ from (32) is determined by the functions of $b(\tau)$ and $\omega_0^2(\tau)$. The function of $b(\tau)$ determines the effect of damping in the evolution

of $a(\tau)$, whereas the oscillation, if it exists at all, depends on both $b'(\tau)$ and $\omega_0^2(\tau)$. The damping is more effective for $b > 0$, while for $b < 0$ it may lead acceleration. Further ω_0^2 may alter its sign in a rapidly oscillating field ϕ . Again at the extrema of $a(\tau)$, the equation (32) gives

$$a''_0 = \frac{K^2}{3}(-\gamma\phi_0'^2 - V_0)a_0 + \frac{\kappa K^2}{2} \frac{\Lambda_0''}{a_0} = \frac{K^2}{3}(\phi_0'^2 - V_0)a_0 + \frac{K^2\Lambda_0}{2a_0}(-\nu\phi_0'' + \nu^2\phi_0'^2)e^{-\nu\phi_0}, \quad (33)$$

for $\kappa = 1$ and $\gamma = -1$. The Gauss Bonnet term is assumed to be a small correction to the gravity, however the second term $\frac{\Lambda_0''}{a_0}$ in (33) may be large in the early universe, while the first term in (33) will be large at later era. The values of $a''(\tau)$ (i.e. either positive or negative) at the extrema are determined by the fluctuating field ϕ , coupling function, and the potential at the extrema.

6 Discussion:

We present some analytic and numerical wormhole solutions in the 4-dimensional Robertson Walker Euclidean background in the Einstein Gauss-Bonnet dilaton theory. Analytic solution in general is not trivial; so the solutions are obtained with simplified assumption for $\kappa = 0$ with a restriction on the coupling function $\Lambda(\phi)$ as $\Lambda' \frac{a'}{a} = \frac{2m}{K^2}$. The problem of the cosmic singularity is avoided in the wormhole configuration with τ . Further, the wormhole in some analytic solutions (subsection 3.2.2) transforms to an exponential expansion with t using $\tau = it$ after crossing a phase of oscillating universe having a deSitter radius.

We here present numerical solution of wormhole with exponential and a few inverse power law potentials with a plot of $a(\tau)$ vs τ . Wormhole solutions with inverse power law potentials depict multiple local maxima and minima about a global minimum at the throat, while for exponential potential, we have usual wormhole of single minimum. The consequence of numerical solution of the wormholes are studied by curve fit of $a(\tau)$ for ϕ^{-2} potential. We evaluate $a(t)$ from fitted polynomial of $a(\tau)$ by analytic continuation $\tau = it$. These are then used to evaluate the Hubble parameter $H(t)$ and the deceleration parameter $q(t)$ to study cosmic scenario of the early universe. These lead to two distinct classes of variables $\{a(t), H(t), q(t)\}$ depending on the fit of $a(\tau)$ either with polynomial of “odd and even” or only “even” power of τ .

The evolution of $H(t)$ (or real part of $H(t)$) shows that the domain $t < t_i$ is the initial collapsing phase, while $t > t_f$ is the expanding (final) phase after evolving through the throat of wormhole and the parameter $H(t)$ (or real part of $H(t)$) shows unusual evolution within domain $t_i \leq t \leq t_f$ around the throat. This unusual regime may be considered as classical forbidden domain. The parameters $H(t)$ and $q(t)$ have both real and imaginary parts when $a(\tau)$ is fitted with polynomial of “odd and even” power of τ . Further the real parts of them dominate over the imaginary parts outside the classical forbidden domain and the imaginary parts of them vanish far away from the classical forbidden domain. Imaginary parts of the parameters $\{H(t), q(t)\}$ are questionable from the observational point of view. But we can alleviate the appearance of imaginary parts of them using fit of $a(\tau)$ with polynomial of only “even” power of τ , though the fit of $a(\tau)$ with “odd and even” power of τ is better one. The plots of $H(t)$ and $q(t)$ evaluated from the fit with polynomial of “even” power of τ are identical with the real parts of $H(t)$ and $q(t)$ obtained from “odd and even” power of τ .

The Hubble parameter $H(t)$ approaches to a constant value far away from the throat (i.e. $t \gg t_f$), and the deceleration parameter $q(t)$ simultaneously approaches to -1 , while the dynamical potential $V(\phi)$ approaches to very small value at $t \gg t_f$. An estimate of decrease of potential yields $\frac{V(\tau=2.7)}{V(\tau=10^{30})} \approx 10^{63}$ and $\frac{V(\tau=2.7)}{V(\tau=10^{65})} \approx 10^{132}$ for $V_0 e^{-\mu\phi}$ potential with initial condition given in black curve of fig.1b. Thus the cosmic scenario of a Euclidean wormhole leads to an exponential expanding universe under analytic continuation by $\tau = it$. We have seen that these results are true for other standard potentials. So it seems that inflationary expansion is a consequence of the wormhole solution in the Euclidean space in the Einstein Gauss-Bonnet dilaton theory. This is the new feature in the literature. We further present wormhole solutions (Appendix-I) with some values of α in the inverse potential $\phi^{-\alpha}$.

7 Appendix

7.1 Appendix-I: Wormhole solution with different potentials but with same initial condition:

It is observed that the numerical solutions allow wormhole configuration with inverse power law potential $\phi^{-\alpha}$ for $\alpha = \frac{5}{2}, \frac{7}{3}, 2, \frac{5}{3}$, etc under same initial condition in each case. These solutions are presented in

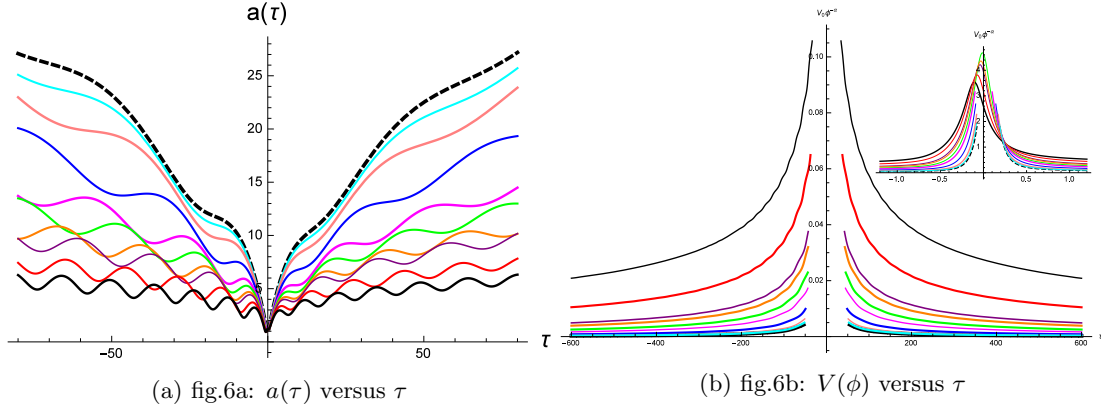


Figure 6: The plot of $a(\tau)$ and $V(\phi)$ with τ are shown respectively in fig.6a and fig.6b using initial conditions $(a(0.1) = 1.2, a'(0.1) = -0.2, \phi(0.1) = 0.5, \phi'(0.1) = 2.2)$ for $V_0\phi^{-\alpha}$ potential with $\gamma = -1$, $V_0 = 1$, $K = 1$, $\kappa = 1$, $\nu = 0.7$ and $\Lambda_0 = 1$. The values of the index α in the plots are $\alpha = 2.6, \frac{5}{2}, \frac{7}{3}, 2, \frac{5}{3}, \frac{3}{2}, \frac{4}{3}, \frac{5}{4}, 1, \frac{4}{5}$ respectively in the black dotted, cyan, pink, blue, magenta, green, orange, purple, red and black curves in fig.5.

the fig.6. It is observed from the numerical solutions that approximate highest value of index α is $\alpha = 2.6$ in $\phi^{-\alpha}$ potential to get wormhole. The scale factor increases to a faster rate for higher values of α .

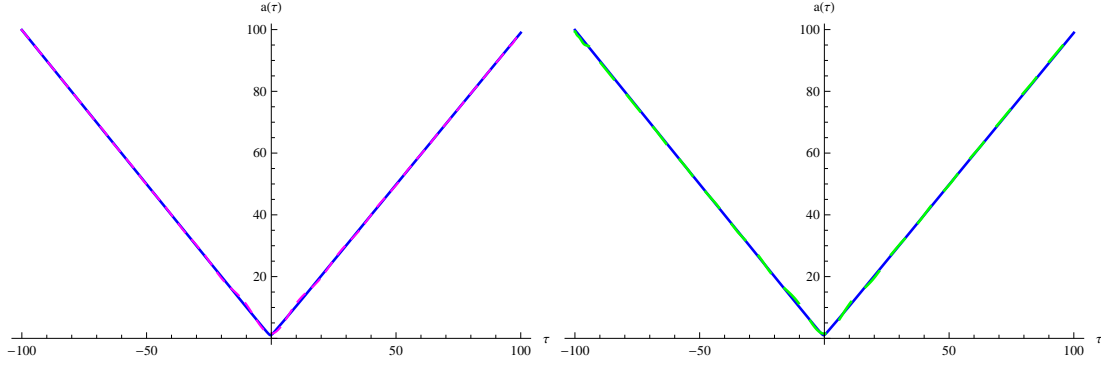
7.2 Appendix-II: Expression of $a(\tau)$ using fit of numerical solution with polynomial in τ :

Again the fit of numerical solution of $a(\tau)$ using polynomial of odd and even power of τ within $-50 \leq \tau \leq 50$ for $V_0\phi^{-2}$ potential with initial condition of fig.3a gives

$$\begin{aligned}
a(\tau) = & 2.23419 - 0.071019\tau + 0.379634\tau^2 + 0.00413109\tau^3 - 0.00800463\tau^4 - 0.0000748033\tau^5 + 0.000090918\tau^6 \\
& + 7.5182179 * 10^{-7}\tau^7 - 6.3204586 * 10^{-7}\tau^8 - 4.8473637 * 10^{-9}\tau^9 + 2.87390304 * 10^{-9}\tau^{10} + \\
& 2.1081491 * 10^{-11}\tau^{11} - 8.9022224 * 10^{-12}\tau^{12} - 6.3825773 * 10^{-14}\tau^{13} + 1.9280816 * 10^{-14}\tau^{14} + 1.3750221 * 10^{-16}\tau^{15} - \\
& 2.9541519 * 10^{-17}\tau^{16} - 2.1307452 * 10^{-19}\tau^{17} + 3.1810737 * 10^{-20}\tau^{18} + 2.3648932 * 10^{-22}\tau^{19} - 2.3169987 * 10^{-23}\tau^{20} - \\
& 1.824845 * 10^{-25}\tau^{21} + 1.0079847 * 10^{-26}\tau^{22} + 8.9222656 * 10^{-29}\tau^{23} - 1.2695245 * 10^{-30}\tau^{24} - 1.8388679 * 10^{-32}\tau^{25} - \\
& 1.0695908 * 10^{-33}\tau^{26} - 6.5039467 * 10^{-36}\tau^{27} + 4.3551887 * 10^{-37}\tau^{28} + 4.7491242 * 10^{-39}\tau^{29} + 9.624324 * 10^{-41}\tau^{30} - \\
& 3.0447219 * 10^{-44}\tau^{31} - 7.70942 * 10^{-44}\tau^{32} - 7.5475389 * 10^{-46}\tau^{33} - 1.049338 * 10^{-47}\tau^{34} + 1.1531204 * 10^{-49}\tau^{35} + \\
& 1.2831719 * 10^{-50}\tau^{36} + 1.0942404 * 10^{-52}\tau^{37} + 1.2491877 * 10^{-54}\tau^{38} - 3.6785252 * 10^{-56}\tau^{39} - 2.2327906 * 10^{-57}\tau^{40} - \\
& 1.1648022 * 10^{-59}\tau^{41} + 7.6027120 * 10^{-63}\tau^{42} + 1.0323276 * 10^{-62}\tau^{43} + 4.0566396 * 10^{-64}\tau^{44} - 2.8878199 * 10^{-66}\tau^{45} - \\
& 1.5074807 * 10^{-67}\tau^{46} + 3.8790993 * 10^{-70}\tau^{47} + 2.3591084 * 10^{-71}\tau^{48} - 2.1208468 * 10^{-74}\tau^{49} - 1.4339072 * 10^{-75}\tau^{50}
\end{aligned} \tag{34}$$

The fit of numerical solution of $a(\tau)$ using polynomial of even power of τ within $-50 \leq \tau \leq 50$ for $V_0\phi^{-2}$ potential with initial condition of fig.3b gives

$$\begin{aligned}
a(\tau) = & 2.23756 + 0.37757\tau^2 - 7.89409 * 10^{-3}\tau^4 + 8.88124 * 10^{-5}\tau^6 - 6.1203496 * 10^{-7}\tau^8 + \\
& 2.76216675 * 10^{-9}\tau^{10} - 8.5021053 * 10^{-12}\tau^{12} + 1.8314958 * 10^{-14}\tau^{14} - 2.7929551 * 10^{-17}\tau^{16} + \\
& 2.9945401 * 10^{-20}\tau^{18} - 2.1715504 * 10^{-23}\tau^{20} + 9.3904486 * 10^{-27}\tau^{22} - 1.1507882 * 10^{-30}\tau^{24} - \\
& 1.0100342 * 10^{-33}\tau^{26} + 4.0420694 * 10^{-37}\tau^{28} + 9.2378076 * 10^{-41}\tau^{30} - 7.2048338 * 10^{-44}\tau^{32} - \\
& 1.0208739 * 10^{-47}\tau^{34} + 1.2047031 * 10^{-50}\tau^{36} + 1.2292825 * 10^{-54}\tau^{38} - 2.1068493 * 10^{-57}\tau^{40} + \\
& 3.160816 * 10^{-64}\tau^{42} + 3.8512670 * 10^{-64}\tau^{44} - 1.4260117 * 10^{-67}\tau^{46} \\
& + 2.2284504 * 10^{-71}\tau^{48} - 1.3534363 * 10^{-75}\tau^{50}
\end{aligned} \tag{35}$$



(a) fig.7a: Plot of $a(\tau)$ (blue curve) and the corresponding fitted dashed magenta curve using fit with polynomial of “odd and even” power of τ for $e^{-\mu\phi}$ potential. (b) fig.7b: The plot of $a(\tau)$ (blue curve) and the corresponding fitted dashed green curve using fit with polynomial of “even” power of τ for $e^{-\mu\phi}$ potential.

Figure 7: The initial conditions in numerical solution of $a(\tau)$ shown in black dashed curve are $\left(a(1) = 1.9, a'(1) = .9, \phi(1) = 0.8, \phi'(1) = -.4\right)$ same as fig.1a with $\gamma = -1, V_0 = 1, K = 1, \kappa = 1, \nu = 1, \mu = 8$ and $\Lambda_0 = 1$.

7.3 Appendix-III: Expression of $a(\tau)$ using fit of numerical solution with polynomial in τ :

Again fit of numerical solution of $a(\tau)$ using polynomial of odd and even power of τ within $-50 \leq \tau \leq 50$ for $V_0 e^{-\mu\phi}$ potential with initial condition of fig.7a gives

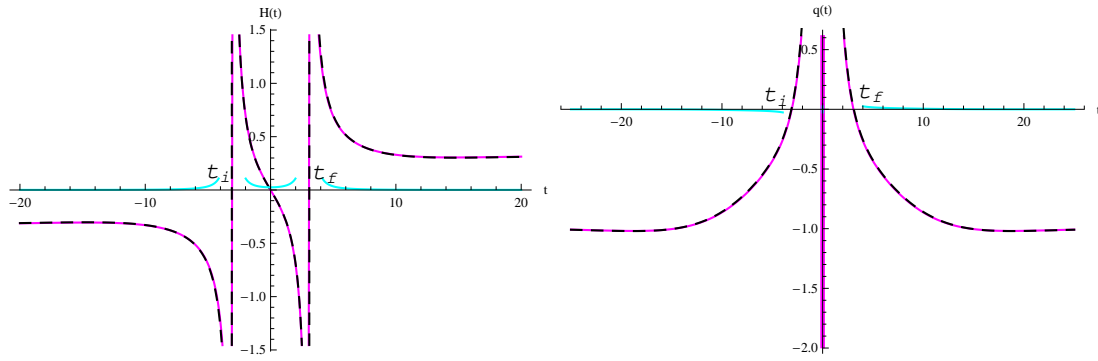
$$\begin{aligned}
a(\tau) = & 1.53331 + 0.0385906\tau + 0.154504\tau^2 - 0.000337597\tau^3 - 0.000794916\tau^4 + 1.29187 * 10^{-6}\tau^5 + 2.53587 * 10^{-6}\tau^6 \\
& - 2.41844 * 10^{-9}\tau^7 - 4.7721 * 10^{-9}\tau^8 + 2.32258 * 10^{-12}\tau^9 + 5.71634 * 10^{-12}\tau^{10} + \\
& - 9.25707 * 10^{-16}\tau^{11} - 4.60595 * 10^{-15}\tau^{12} - 3.20447 * 10^{-19}\tau^{13} + 2.58307 * 10^{-18}\tau^{14} + 6.18452 * 10^{-22}\tau^{15} - \\
& - 1.02476 * 10^{-21}\tau^{16} - 3.77939 * 10^{-25}\tau^{17} + 2.868 * 10^{-25}\tau^{18} + 1.35796 * 10^{-28}\tau^{19} - 5.48544 * 10^{-29}\tau^{20} - \\
& - 3.11725 * 10^{-32}\tau^{21} + 6.46997 * 10^{-33}\tau^{22} + 4.38532 * 10^{-36}\tau^{23} - 2.89697 * 10^{-37}\tau^{24} - 2.78165 * 10^{-40}\tau^{25} - \\
& 3.25138 * 10^{-41}\tau^{26} - 1.62832 * 10^{-44}\tau^{27} + 4.4815 * 10^{-45}\tau^{28} + 3.97427 * 10^{-48}\tau^{29} + 1.26388 * 10^{-49}\tau^{30} - \\
& - 5.25962 * 10^{-53}\tau^{31} - 4.49476 * 10^{-53}\tau^{32} - 3.82583 * 10^{-56}\tau^{33} - 5.90006 * 10^{-58}\tau^{34} + 1.8603 * 10^{-60}\tau^{35} + \\
& + 4.43797 * 10^{-61}\tau^{36} + 3.44701 * 10^{-64}\tau^{37} + 3.03464 * 10^{-66}\tau^{38} - 3.31041 * 10^{-68}\tau^{39} - 4.59791 * 10^{-69}\tau^{40} - \\
& 2.21357 * 10^{-72}\tau^{41} + 6.31847 * 10^{-74}\tau^{42} + 5.53121 * 10^{-76}\tau^{43} + 4.8687 * 10^{-77}\tau^{44} - 4.03764 * 10^{-80}\tau^{45} - \\
& 4.86454 * 10^{-81}\tau^{46} + 1.40241 * 10^{-84}\tau^{47} + 1.96883 * 10^{-85}\tau^{48} - 1.97833 * 10^{-89}\tau^{49} - 3.05922 * 10^{-90}\tau^{50}
\end{aligned} \tag{36}$$

The fit of numerical solution of $a(\tau)$ using polynomial of even power of τ within $-50 \leq \tau \leq 50$ for $V_0 e^{-\mu\phi}$ potential with initial condition of fig.7b gives

$$\begin{aligned}
a(\tau) = & 1.5275 + 0.1514\tau^2 - 0.00076\tau^4 + 2.3941 * 10^{-6}\tau^6 - 4.4594 * 10^{-9}\tau^8 + \\
& + 5.2963 * 10^{-12}\tau^{10} - 4.23510 * 10^{-15}\tau^{12} + 2.35826 * 10^{-18}\tau^{14} - 9.29160 * 10^{-22}\tau^{16} + \\
& 2.58246 * 10^{-25}\tau^{18} - 4.90201 * 10^{-29}\tau^{20} + 5.72424 * 10^{-33}\tau^{22} - 2.49059 * 10^{-37}\tau^{24} - \\
& 2.94192 * 10^{-41}\tau^{26} + 3.92669 * 10^{-45}\tau^{28} + 1.19820 * 10^{-49}\tau^{30} - 3.958594 * 10^{-53}\tau^{32} - \\
& 5.99864 * 10^{-58}\tau^{34} + 3.91734 * 10^{-61}\tau^{36} + 3.38699 * 10^{-66}\tau^{38} - 4.06910 * 10^{-69}\tau^{40} + \\
& 5.00345 * 10^{-74}\tau^{42} + 4.33577 * 10^{-77}\tau^{44} - 4.29249 * 10^{-81}\tau^{46} + 1.72956 * 10^{-85}\tau^{48} - 2.67925 * 10^{-90}\tau^{50}
\end{aligned} \tag{37}$$

References

- [1] A Guth, Phys. Rev. D, **23** 347 (1981)



(a) fig.8a: Plot of $H(t)$ versus t for $e^{-\mu\phi}$ potential. (b) fig.8b: Plot of $q(t)$ versus t for $e^{-\mu\phi}$ potential.

Figure 8: The evolution of $H(t)$ and $q(t)$ with t are shown respectively in fig.8a and fig.8b. Real and imaginary parts of $H(t)$ and $q(t)$ obtained from the fit of $a(\tau)$ with polynomial of “odd and even” power of τ are shown respectively in magenta and cyan curves. Again fit of $a(\tau)$ with polynomial of “even” power of τ leads to real $H(t)$ and $q(t)$, which are shown by dashed curves.

- [2] A D Linde, Phys. Lett. B, **108** 389 (1982)
- [3] A Albrecht and P J Steinhardt, Phys. Rev. Lett., **48** 1220 (1982)
- [4] A Starobinsky, Phys. Lett. B, **117** 175 (1982)
- [5] T Padmanavan, “Structure formation in the universe”, Cambridge University Press, Cambridge, England, (1993)
- [6] K S Stelle, Phys. Rev. D, **16** 953 (1977)
- [7] S Capozziello, T Harko, T S Koivisto, F S N Lobo and G J Olmo, Phys. Rev. D, **86** 127504 (2012)
- [8] T Harko, F S N Lobo, M K Mak and S V Sushkov, Phys. Rev. D, **87** 067504 (2013)
- [9] F S N Lobo and M A Oliveira, Phys. Rev. D, **80** 104012 (2009)
- [10] D J Gross and J H Sloan, Nucl. Phys. B, **291** 41 (1987)
- [11] R R Metsaev and A A Tseytlin, Nucl. Phys. B, **293** 385 (1987)
- [12] V Dzhumushaliev and D Singleton, Phys. Rev. D, **59** 064018 (1999)
- [13] K Sarkar, G Biswas and B Modak, Gen. Rel. Grav., **50** 157 (2018)
- [14] I P Neupane and B M N Carter, JCAP, **0606** 004 (2006)
- [15] S Tsujikawa and M Sami, JCAP, **0701** 006 (2007)
- [16] P Kanti, J Rizos and K Tamvakis, Phys. Rev. D, **59** 083512 (1999)
- [17] I Antoniadis, J Rizos and K Tamvakis, Nucl. Phys. B, **415** 497 (1994)
- [18] X Y Chew, G Tumurtushaa and D H Yeom, Physics of the Dark Universe, **32** 100811 (2021)
- [19] G Tumurtushaa and D Yeom, Eur. Phys. J. C, **79** 488 (2019)
- [20] S Coleman, Nucl. Phys. B, **310** 643 (1988)
- [21] E Baum, Phys. Lett. B, **133** 185 (1983)
- [22] S W Hawking, Phys. Lett. B, **134** 403 (1984)
- [23] S Giddings and A Strominger, Nucl.Phys. B, **306** 890 (1988)
- [24] M S Morris and K S Thorne, Am J Phys, **56** 395 (1988)
- [25] M S Morris, K S Thorne and U Yurtsever, Phys. Rev. Lett., **61** 1446 (1988)

- [26] J Halliwell and R Laflamme, *Class. Quant. Grav.*, **6** 1839 (1989)
- [27] D H Coule and K I Maeda, *Class. Quant. Grav.*, **7** 955 (1990)
- [28] F S N Lobo and M Oliviera, *Phys. Rev. D*, **81** 067501 (2010)
- [29] K K Nandi, B Bhattacharjee, S M K Alam and J Evans, *Phys. Rev. D*, **57** 823 (1998)
- [30] S W Hawking, *Phys. Rev. D*, **37** 904 (1988)
- [31] S B Giddings and A Strominger, *Nucl. Phys. B*, **307** 854 (1988)
- [32] W Fischler and L Susskind, *Phys. Lett. B*, **217** 48 (1989)
- [33] W J Unruh, *Phys. Rev. D*, **40** 1053 (1989)
- [34] S W Hawking, *Nucl. Phys. B*, **335** 155 (1990)
- [35] S W Hawking and D N Page, *Phys. Rev. D*, **42** 2665 (1990)
- [36] I Klebanov, L Susskind and T Banks, *Nucl. Phys. B*, **317**, 665 (1989)
- [37] M Visser, S Kar and N Dadhich, *Phys. Rev. Lett.*, **90**, 201102 (2003)
- [38] L Z Fang and M Li, “ Formation of Black Holes in Quantum Cosmology”, International Centre for Theoretical Physics, (1985)
- [39] N D Birrel and P C W Davis, “ Quantum Fields in curved Space”, Cambridge University Press, Cambridge, England, (1982)
- [40] P Kanti, B Kleihaus and J Kunz, *Phys. Rev. Lett.*, **107** 271101 (2011)
- [41] M R Mehdizadeh, M K Zangeneh and F S N Lobo, *Phys. Rev. D*, **91** 084004 (2015)
- [42] B Bhawal and S Kar, *Phys. Rev. D*, **46** 2464 (1992)
- [43] G Biswas and B Modak, (*communicated*)
- [44] G Biswas, K Sarkar and B Modak, *Mod. Phys. Lett. A*, **36** 2150107 (2021)
- [45] G Biswas and B Modak, *Mod. Phys. Lett. A*, **32** 7, 1750023 (2017)
- [46] B Ratra and P J Peebles, *Phys. Rev. D*, **37** 3406 (1988)
- [47] S Ruz, et al., *Class. Quant. Grav.*, **30** 175013 (2013)
- [48] S Nojiri, S D Odintsov and M Sasaki, *Phys. Rev. D*, **71** 123 (2005)
- [49] M R Mehdizadeh, *Euro.Phys.J.C*, **80** 310 (2020)
- [50] P Chen and D Yeom, *Euro.Phys.J.C*, **78** 863 (2018)
- [51] B. C. Paul et al, *Pramana-Journal of Physics*, **44** 133 (1995)
- [52] S Koh, B H Lee and G Tumurtushaa, *Phys. Rev. D*, **95** 123509 (2017)
- [53] M K Dutta and B Modak, *Int. J. Theor. Phys*, **54** 2591 (2015)
- [54] R N Bose and B Modak, *Int. J. Theor. Phys*, **51** 350 (2012)
- [55] A Carlini, D H Coule and D M Solomons, *NORDITA-94/75A*(1994)
- [56] B Modak and G Biswas, *communicated*, arXiv: 2111.10820 [gr-qc](2021)
- [57] I P Neupane, *Class. Quant. Grav.*, **23** 7493 (2006)
- [58] R R Caldwell, *Phys. Lett. B*, **545** 23 (2002)
- [59] T Biswas and A Mazumder, *Phys. Rev. D*, **80** 023519 (2009)